Acta Astronautica 198 (2022) 152–160

Contents lists available at ScienceDirect

Acta Astronautica

journal homepage: www.elsevier.com/locate/actaastro

Performance analysis of impulsive station-keeping strategies for *cis*-lunar orbits with the ephemeris model

Ruikang Zhang [a], Yue Wang [a,*], Yu Shi [b], Chen Zhang [b], Hao Zhang [b]

[a] School of Astronautics, Beihang University, Beijing, 102206, China
[b] Technology and Engineering Center for Space Utilization, Chinese Academy of Sciences, Beijing, 100094, China

ARTICLE INFO

Keywords:
Station-keeping
The Earth-Moon system
Ephemeris model
Near rectilinear halo orbits
Distant retrograde orbits
Halo orbits

ABSTRACT

Future long-term lunar missions, such as *cis*-lunar space stations and communication/navigation constellations, have been proposed by different space agencies. For such long-term missions, reliable station-keeping strategies are of great importance to counteract unfavourable effects of perturbations, navigation errors, etc. In this study, representative *cis*-lunar orbits with favourable characteristics, including near rectilinear halo orbits (NRHOs), distant retrograde orbits (DROs), and halo orbits, are considered as nominal orbits of long-term lunar missions for station-keeping analysis. Both the target point method and the discrete linear quadrant regulator (DLQR) control are applied to these nominal orbits in the ephemeris model. Under some practical constraints caused by the navigation and orbital control systems, Monte-Carlo simulations are carried out to evaluate performances of the station-keeping strategies. Then, effects of solar radiation pressure (SRP) and nonspherical lunar gravity on the station-keeping performances are demonstrated by Monte-Carlo simulations with low-fidelity nominal orbits constructed in ephemeris models without SRP or nonspherical lunar gravity. Finally, comparisons between different impulse intervals are made to find the balance between the station-keeping cost and position deviation. It is found that the stability index of the nominal orbit has no direct effect on the station-keeping cost, but plays an important role in the selection of the impulse interval. The DROs and NRHOs allow a much longer impulse interval than the unstable halo orbits. The results can provide useful references for selections of the nominal orbit and station-keeping strategy in future long-term lunar missions.

1. Introduction

Long-term lunar missions, such as *cis*-lunar space stations and communication/navigation constellations, require reliable station-keeping strategies to counteract unfavourable effects of perturbations, navigation errors, etc. The performance analysis of station-keeping strategies is important for the nominal orbit selection and the mission design. So far, the periodic orbits with favourable characteristics in *cis*-lunar space, such as near rectilinear halo orbits (NRHOs) and distant retrograde orbits (DROs), have been considered as potential nominal orbits for future long-term missions.

The studies of NRHOs and DROs began quite early. In the 1970s, Lidov [1] and Breakwell and Brown [2] independently discovered the NRHOs, which are subsets of the halo orbit families. Due to their stable or marginally unstable characteristics, the NRHOs have been considered as parking orbits for the Deep Space Gateway (DSG), a crewed lunar space station mission proposed by NASA. The investigations of NRHOs have been conducted in various aspects, such as dynamical features, station-keeping strategy, rendezvous design, navigation challenges, eclipse condition, and transfer problems [3–11]. Another type of potential nominal orbits, the DROs, are planar periodic orbits in retrograde motion around the Moon. The DRO family was discovered in the 1960s by Broucke [12] and Hénon [13]. As with the NRHOs, various aspects of the DROs have already been investigated by researchers, mostly focused on dynamical features and transfer problems [11,14–19]. However, the station-keeping of DROs has not been discussed comprehensively. Although NRHOs and DROs have favourable stability, the position deviation caused by perturbations is still unavoidable during the long-term lunar missions, and thus a proper station-keeping strategy is necessary to maintain the real trajectory close to the desired nominal orbit.

The station-keeping problem has been a continual research topic in the past decades, while most researchers focused on the libration point

* Corresponding author.
E-mail addresses: zhangruikang@buaa.edu.cn (R. Zhang), ywang@buaa.edu.cn (Y. Wang), shiyu@csu.ac.cn (Y. Shi), chenzhang.buaa@gmail.com (C. Zhang), hao.zhang.zhr@gmail.com (H. Zhang).

https://doi.org/10.1016/j.actaastro.2022.05.054
Received 25 January 2022; Received in revised form 24 April 2022; Accepted 31 May 2022
Available online 3 June 2022

orbits [4,5,10,20–29]. The station-keeping strategies can be classified into two categories based on the thrust type, impulsive and continuous. Currently, station-keeping strategies with impulsive thrust are considered more practical. Different station-keeping strategies with impulsive thrust have been proposed based on dynamical properties and control theory. The target point method developed by Howell and Pernicka discretizes the nominal orbit as a serious of points with different epochs, and defines them as target points [23]. By minimizing the performance function constructed by the position deviation and station-keeping cost at predefined target points, the balance between the deviation and cost is achieved. Another classic station-keeping strategy is the Floquet mode approach, which was proposed by Wiesel and Shelton [20], Simó et al. [21], and Gómez et al. [22]. The approach aims to apply a station-keeping impulse to counteract the unstable mode of periodic orbits. Lian et al. proposed a discrete-time sliding mode control (DSMC) based on the discrete dynamic model, and verified it with both halo orbits and Lissajous orbits, using the discrete linear quadratic regulator (DLQR) control as a comparison [26]. The strategy called Cauchy-Green Tensor (CGT) targeting approach was developed by Guzzetti et al. in the investigation of NRHOs station-keeping [3]. The CGT targeting approach utilizes the state transition matrix to construct the CGT matrix, and then the accessible region under the linear approximation is obtained by using the eigenvectors of the CGT matrix. Shirobokov et al. comprehensively reviewed previous station-keeping techniques for libration point orbits and provided some valuable suggestions [27].

Previous studies have given several guidelines for the station-keeping strategy construction and verification. The nominal orbits should be constructed in a high-fidelity model, since much higher station-keeping cost will be required to counteract neglected perturbations for nominal orbits constructed in a low-fidelity model. To verify the effectiveness of a station-keeping strategy, Monte-Carlo simulations are generally required to provide reliable results. Besides, nonspherical lunar gravity needs to be considered for orbits with a low perilune, such as NRHOs [3].

In this paper, the station-keeping problem of *cis*-lunar orbits is investigated in the ephemeris model under some practical constraints. Several representative *cis*-lunar orbits, including DROs, halo orbits, and NRHOs, are constructed in the full ephemeris model as nominal orbits. The target point method and the DLQR control are then carefully set and applied to these nominal orbits. Under some practical constraints caused by the navigation and orbital control system, Monte-Carlo simulations are carried out to analysis the performance of station-keeping strategies. Then, the ephemeris models without solar radiation pressure (SRP) or nonspherical lunar gravity are constructed to obtain the corresponding nominal orbit, and the effects of these perturbations on the station-keeping performance are demonstrated. Since both the NRHOs and DROs have favourable stability, longer impulsive intervals are also considered. Station-keeping simulations with different impulse intervals are conducted to find the delicate balance between station-keeping cost and position deviation.

2. Background

In this section, the circular restricted three body problem (CR3BP) and the high-fidelity ephemeris model are both introduced, and the nominal orbits in the *cis*-lunar space are finally constructed in the ephemeris model.

2.1. Circular restricted three-body problem

The CR3BP is a classic dynamical model for spacecraft in the Earth-Moon system. The spacecraft is assumed to be massless and attracted by the gravity of the Earth and the Moon, while the Earth and the Moon are assumed to be in circular motions around their barycenter. The motion of the spacecraft is described in a synodic frame, which has its origin at the barycenter of the Earth-Moon system. The $\boldsymbol{x}$-axis is pointing towards the Moon, the $\boldsymbol{z}$-axis aligns along the angular momentum, and the $\boldsymbol{y}$-axis is determined by the right-hand rule. The masses of the Earth and the Moon are denoted by m_1 and m_2, respectively, and the equations of motion of the spacecraft can be expressed as

$$\begin{aligned} \ddot{x} - 2\dot{y} &= \frac{\partial \Omega_3}{\partial x} \\ \ddot{y} + 2\dot{x} &= \frac{\partial \Omega_3}{\partial y}, \\ \ddot{z} &= \frac{\partial \Omega_3}{\partial z} \end{aligned} \tag{1}$$

where $[x, y, z, \dot{x}, \dot{y}, \dot{z}]$ is the location and velocity of the spacecraft, and the effective potential Ω_3 is expressed as

$$\Omega_3 = \frac{1}{2}\left(x^2 + y^2\right) + \frac{1-\mu}{r_1} + \frac{\mu}{r_2} + \frac{1}{2}\mu(1-\mu). \tag{2}$$

In Eq. (2), $\mu = m_2/(m_1 + m_2) = 1.21506683 \times 10^{-2}$ is the mass ratio of the Earth-Moon system, r_1 and r_2 are the distances between the spacecraft and each of the primaries, expressed as $r_1 = \left[(x+\mu)^2 + y^2 + z^2\right]^{1/2}$ and $r_2 = \left[(x+\mu-1)^2 + y^2 + z^2\right]^{1/2}$, respectively.

2.2. Ephemeris model

The ephemeris model is constructed based on the classic restricted N-body problem, and the Moon-centred J2000 inertial coordinates is used here to study the orbital motion of spacecraft, as shown in Fig. 1. The equation of motion of the spacecraft in the Moon-centred J2000 inertial frame is expressed as

$$\ddot{\boldsymbol{r}}_{\boldsymbol{cs}} = -\frac{Gm_c}{r_{cs}^3}\boldsymbol{r}_{cs} - G\sum_{\substack{j=1 \\ j\neq s,c}}^{n} m_j\left(\frac{\boldsymbol{r}_{sj}}{r_{sj}^3} - \frac{\boldsymbol{r}_{cj}}{r_{cj}^3}\right) + \boldsymbol{a}_{\boldsymbol{SRP}}, \tag{3}$$

where $\boldsymbol{r}_{\boldsymbol{cs}}$ is the position vector from the central body to the spacecraft, and $\boldsymbol{r}_{\boldsymbol{sj}}, \boldsymbol{r}_{\boldsymbol{cj}}$ are the position vector from the spacecraft and the central body to other bodies, respectively.

The SRP acceleration is denoted as $\boldsymbol{a}_{\boldsymbol{SRP}}$, which can be obtained by using the cannonball model [30].

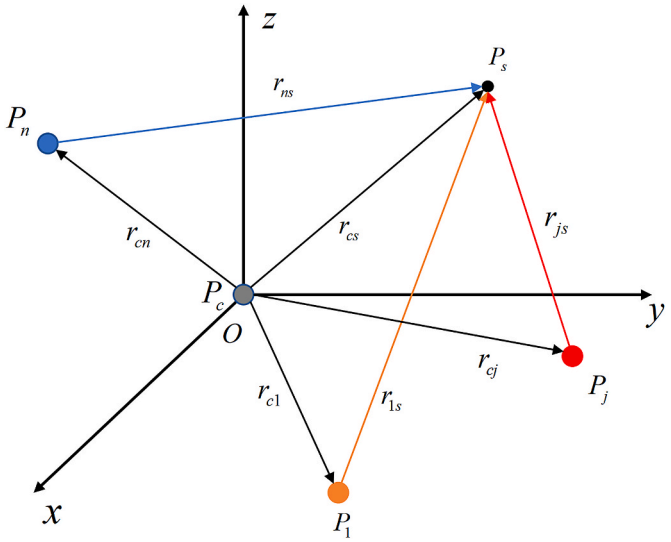

Fig. 1. The orbital motion of spacecraft in the full ephemeris model.

$$\boldsymbol{a}_{SRP} = \frac{P_{SRP} C_r A}{m} \boldsymbol{r}_{S-sat}, \tag{4}$$

$$P_{SRP} = \frac{P_0}{c}\left(\frac{R_0}{R}\right)^2, C_r = 1 + \rho_s + \frac{5}{3}\rho_d, \tag{5}$$

where A, m are the surface area and the mass of the spacecraft, $\boldsymbol{r}_{S-sat}$ is the position unit vector from the Sun to the spacecraft, $P_0 = 1367\mathrm{W}/\mathrm{m}^2$ is a characteristic constant, c is the speed of light, R_0 is the distance between the Sun and the Earth, ρ_s, ρ_d are the reflection and scattering rates of the spacecraft, and ρ_d is normally considered to be zero. In this study, the mass, the surface area, and the reflectivity of the spacecraft are 1850 kg, 34.675 m^2, and 0.9, respectively.

In this study, the Moon is selected as the central body, and the Earth, the Sun, and the Jupiter are incorporated in the ephemeris model as perturbing bodies. The relative position of each perturbing body with respect to the Moon is instantaneously obtained by employing the NAIF SPICE software and the DE438 file. Since the perilunes of the NRHOs are close to the Moon, the lunar gravity field is modelled using the spherical harmonics truncated to degree and order 8, and the coefficients in the GRAIL (GRGM660PRIM) model are used here.

2.3. Nominal orbits

The NRHOs and DROs are both considered as potential nominal orbits for long-term lunar missions. To get more comprehensive results, five DROs denoted as the DRO (1)–(5), five halo orbits denoted as the halo (1)–(5) orbit, and five NRHOs denoted as the NRHO (1)–(5) are considered as nominal orbits, which are all obtained in the CR3BP by using differential correction. Fig. 2 shows the nominal orbits in the CR3BP, and their orbital characteristics are listed in Table 1. In order to be concise, the 2:1 DRO, the halo (3) orbit, and the 9:2 NRHO are used as main nominal orbits, and other nominal orbits are used only to demonstrate station-keeping performances of different orbit families. The 2:1 DRO is the DRO (5), and the 9:2 NRHO is the NRHO (4). The 2:1 DRO means that the spacecraft is at a 2:1 sidereal resonance with the Moon. The 9:2 NRHO is the potential nominal orbit in the Artemis program. For NRHOs, the designation 9:2 means that the spacecraft is at a 9:2 synodic resonance with the Moon. The Moon's sidereal period and synodic periods are approximately 27.322 and 29.531 days, respectively. The main nominal orbits are represented by the black lines, while other nominal orbits are represented by the blue lines.

The stability of periodic orbits can be evaluated by the eigenvalues of their monodromy matrix, and the stability index is defined as

$$\nu = \frac{1}{2}\left(|\lambda_{\max}| + \left|\frac{1}{\lambda_{\max}}\right|\right), \tag{6}$$

where $\lambda_{\max}$ is the eigenvalue of the monodromy matrix with the largest modulus. Since periodic orbits always have a pair of eigenvalues equal to 1, the stability index of periodic orbits must satisfy $\nu \geq 1$. When the stability index is equal to 1, the periodic orbit is considered to be stable. When the stability index is larger than 1, the periodic orbit is considered to be unstable, and the stable and unstable manifolds exist, which play an important role in the transfer design. The stability index can provide meaningful reference in the analysis of station-keeping performances.

Table 1
The characteristics of the selected nominal orbits in the CR3BP.

Orbit	No.	x (nd)	z (nd)	$\dot{y}$ (nd)	Period (days)	Stability index
DRO	1	1.076	0	−0.471	5.464	1
	2	1.098	0	−0.460	7.285	1
	3	1.120	0	−0.462	9.107	1
	4	1.141	0	−0.471	10.928	1
	5	1.175	0	−0.494	13.660	1
halo	1	1.172	−0.086	−0.188	14.583	349.022
	2	1.155	−0.137	−0.214	14.050	138.048
	3	1.136	−0.169	−0.225	13.349	51.584
	4	1.119	−0.187	−0.225	12.573	20.834
	5	1.105	−0.197	−0.219	11.771	17.326
NRHO	1	1.056	−0.198	−0.166	8.597	1.570
	2	1.046	−0.195	−0.149	7.956	1.693
	3	1.037	−0.191	−0.134	7.457	1.641
	4	1.022	−0.182	−0.103	6.562	1.319
	5	1.014	−0.176	−0.086	6.130	1.090

The nominal orbits in the CR3BP cannot be directly used as references for the station-keeping problem, since the CR3BP is a low-fidelity dynamical model and neglects important perturbations. It is necessary to reconstruct the nominal orbits in the full ephemeris model. Several numerical methods of transitioning from the CR3BP to the ephemeris model, such as differential correction [3], two-level corrections [32], forward-backward shooting method [33], and receding horizon targeting [33], have been successfully used in previous studies. All these methods have respective advantages and disadvantages. The differential correction and the receding horizon targeting method are employed here. The NRHOs with years of duration are hard to obtain in the ephemeris model by using the differential correction method, and the receding horizon targeting method is used instead. It is worth mentioning that small discontinuities in velocity (less than 1 mm/s per rev) exist in the NRHOs obtained by the receding horizon targeting method. The nominal orbits refined in the ephemeris model are shown in Fig. 3. The characteristics of nominal orbits in the Moon-centred J2000 frame are listed in Table 2.

3. Station-keeping strategies

In this section, the station-keeping strategies used in our study are introduced, including the target point method and the DLQR control.

3.1. Target point method

The target point method defines the target points by discretizing the

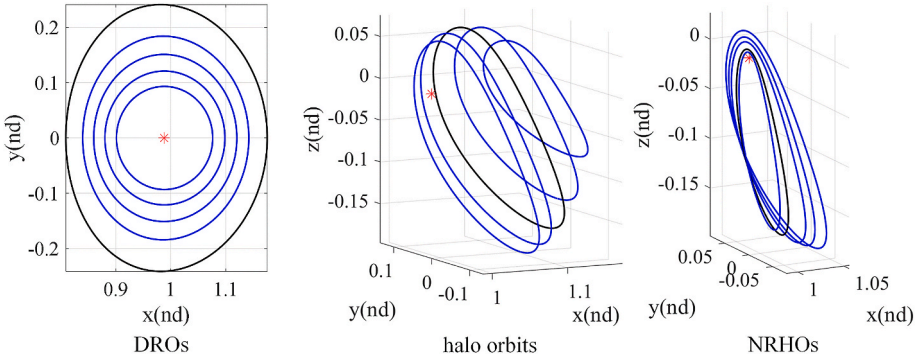

Fig. 2. The nominal orbits in the CR3BP.

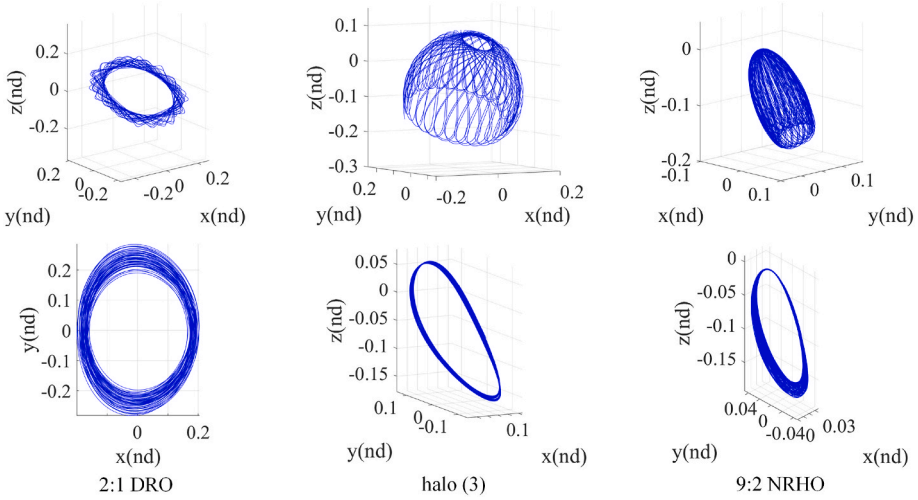

Fig. 3. Three main nominal orbits in the Moon-centred inertial frame and the Moon-centred rotating frame.

Table 2
The characteristics of the refined nominal orbits in the Moon-centred J2000 frame.

Orbit	epoch	x (km)	y (km)	z (km)	$\dot{x}$ (km/s)	$\dot{y}$ (km/s)	$\dot{z}$ (km/s)
2:1 DRO	'2023 SEP 17 20:31:57.99'	−68199.45	−13688.95	−4653.53	−0.0742	0.2640	0.1449
9:2 NRHO	'2023 SEP 17 11:58:53.09'	−15118.12	33384.91	−38118.07	0.0214	−0.0879	0.2380
halo (3)	'2023 SEP 17 12:34:13.28'	−65241.84	35926.69	−42963.88	−0.0070	−0.0233	0.1317

nominal orbit as a serious of points at different epochs. After the current deviation is determined, the deviation of position and velocity at the following target points can be predicted by exploiting the state transition matrix using

$$\begin{bmatrix} \boldsymbol{p}_{k+1} \\ \boldsymbol{v}_{k+1} \end{bmatrix} = \boldsymbol{\varphi}(t_{k+1}, t_k) \begin{bmatrix} \boldsymbol{p}_k \\ \boldsymbol{v}_k + \boldsymbol{\Delta V} \end{bmatrix}, \tag{7}$$

where the state transition matrix can be expressed as

$$\boldsymbol{\varphi}(t_{k+1}, t_k) = \begin{bmatrix} \boldsymbol{A}_k^{k+1} & \boldsymbol{B}_k^{k+1} \\ \boldsymbol{C}_k^{k+1} & \boldsymbol{D}_k^{k+1} \end{bmatrix}. \tag{8}$$

Then, by considering the future position deviation $\boldsymbol{p}_{k+1}$ as zero, the station-keeping impulse of the simplest target point method can be given as

$$\boldsymbol{\Delta V} = -\left(\boldsymbol{B}_k^{k+1}\right)^{-1}\left(\boldsymbol{A}_k^{k+1}\boldsymbol{p}_k + \boldsymbol{B}_k^{k+1}v_k\right). \tag{9}$$

Such a method considers only the position deviation, and no minimization of station-keeping cost is included. Then, by defining the performance index with consideration of the station-keeping impulse and future deviations, another target point method is obtained [23].

$$J(\boldsymbol{p_0}, \boldsymbol{v_0}, \boldsymbol{\Delta V}) = \boldsymbol{\Delta V}^T \boldsymbol{Q} \boldsymbol{\Delta V} + \sum_{i=1}^{n} \left\{ \boldsymbol{p_i}^T \boldsymbol{R_i} \boldsymbol{p_i} + \boldsymbol{v_i}^T \boldsymbol{S_i} \boldsymbol{v_i} \right\}, \tag{10}$$

where $\boldsymbol{Q}$ is a positive definite matrix, and $\boldsymbol{R_i}, \boldsymbol{S_i}$ are positive semi-definite matrixes. The derivative of the performance index is

$$\frac{\partial}{\partial \boldsymbol{\Delta V}} J(\boldsymbol{p_0}, \boldsymbol{v_0}, \boldsymbol{\Delta V}) = \boldsymbol{0}. \tag{11}$$

Here we consider the position deviations of two future target points, the station-keeping impulse is obtained as

$$\Delta V = -\left[Q + B_{10}^T R_1 B_{10} + B_{20}^T R_2 B_{20}\right]^{-1}\left[\left(B_{10}^T R_1 B_{10} + B_{20}^T R_2 B_{20}\right) v_0 + \left(B_{10}^T R_1 A_{10} + B_{20}^T R_2 A_{20}\right) p_0\right], \tag{12}$$

and the parameter matrixes are considered as $\boldsymbol{Q} = \boldsymbol{I}_3$, $\boldsymbol{R}_1 = \boldsymbol{R}_2 = 10\boldsymbol{I}_3$.

3.2. DLQR control

The LQR control is a classic control theory, and has been studied in various fields, including the station-keeping problem. The discrete dynamical model can be expressed as

$$\boldsymbol{x}(k+1) = \boldsymbol{A}\boldsymbol{x}(k) + \boldsymbol{B}\triangle \boldsymbol{v}(k), \tag{13}$$

where

$$\boldsymbol{A} = \boldsymbol{\varphi}(t_{k+1}, t_k), \boldsymbol{B} = \boldsymbol{\varphi}(t_{k+1}, t_k)\overline{\boldsymbol{B}}. \tag{14}$$

In Eq. (14), $\boldsymbol{\varphi}(t_{k+1}, t_k)$ is the state transition matrix, and $\overline{\boldsymbol{B}} =$

$[\mathbf{0}_{3\times3} \quad \boldsymbol{I}_{3\times3}]^T$.

The performance index in Lian et al. is defined as [26].

$$J=\sum_{i=0}^{N-1}\left(\boldsymbol{x}_i^T\boldsymbol{Q}\boldsymbol{x}_i+\triangle\boldsymbol{v}_i^T\boldsymbol{R}\triangle\boldsymbol{v}_i\right)+\boldsymbol{x}_N^T\boldsymbol{Q}_N\boldsymbol{x}_N, \tag{15}$$

where $\boldsymbol{Q}$ and $\boldsymbol{Q}_N$ are positive semi-definite matrixes, and $\boldsymbol{R}$ is a positive definite matrix.

Then, the station-keeping impulse can be obtained by using the following steps:

1) $\boldsymbol{P}_N = \boldsymbol{Q}_N$

2) For $i = N, \cdots, 1$

$$P_{i-1}=A^TP_iA-A^TP_iB\left(R+B^TP_iB\right)^{-1}B^TP_iA+Q$$

3) For $i = N-1, \cdots, 1$

$$K_i=-\left(R+B^TP_{i+1}B\right)^{-1}B^TP_{i+1}A$$

4) For $i = 0, \cdots, N-1$

$$\Delta v_i=K_ix_i$$

The parameter matrixes are considered as $\boldsymbol{Q}=\boldsymbol{Q}_N=\boldsymbol{I}_6$ and $\boldsymbol{R}=5\boldsymbol{I}_3$. It is worth mentioning that the first three steps can be calculated and stored in advance.

Besides the above procedure, another performance index with an infinite-form can be defined for the DLQR control,

$$J=\sum_{i=1}^{\infty}\left(x_i^TQx_i+\triangle v_i^TR\triangle v_i\right) \tag{16}$$

By solving the Ricatti equation,

$$P_i=A^TP_iA-\left(A^TP_iB\right)\left(B^TP_iB+R\right)^{-1}\left(A^TP_iB\right)^T+Q, \tag{17}$$

at each target point, the station-keeping impulse at current target point is obtained as

$$\Delta v_i=-\left(R+B^TPB\right)^{-1}B^TPAx_i. \tag{18}$$

The parameter matrixes in Eq. (18) are also considered as $\boldsymbol{Q}=\boldsymbol{I}_6$ and $\boldsymbol{R}=5\boldsymbol{I}_3$ for comparison.

4. Station-keeping performance evaluation

In this section, several practical constraints in the station-keeping problem are introduced, and station-keeping strategies for different nominal orbits are evaluated by using Monte-Carlo simulations. Some perturbations in the full ephemeris model are focused, and their effects on the station-keeping performances are demonstrated. Finally, different impulse intervals are tested for station-keeping.

4.1. Practical constraints

In real mission scenarios, the capability of the navigation and orbital control system are limited, and then some practical constraints are necessary to consider in the station-keeping verification simulations. The first constraint considered here is that the initial insertion cannot be precisely executed, and the position and velocity of the spacecraft cannot match the nominal orbit precisely. The magnitude of initial insertion errors on the position and velocity are considered to be 10 km and 1 cm/s respectively in this investigation.

The second constraint is that the navigation system cannot provide real-time information about the position and velocity, and so the navigation interval Δt is considered to be 2 days in the station-keeping simulation. The navigation interval Δt represents the time between the measurement instants, which is also the time between station-keeping impulses. The navigation errors on the position and velocity are also nonnegligible limitations, whose magnitudes are considered to be 1 km and 1 cm/s, respectively. After the position and velocity of spacecraft are determined, the station-keeping impulse will be calculated and executed. Since the orbital control system cannot provide the accuracy maneuver, the magnitude of the maneuver error is assumed to be 1%. The minimum maneuver is also considered for the orbital control system, and has the form

$$\Delta\boldsymbol{v}_{real}=\begin{cases}\mathbf{0} & if \quad \|\Delta\boldsymbol{v}\|<\Delta v_{\min}\\ \Delta\boldsymbol{v} & if \quad \|\Delta\boldsymbol{v}\|\geq\Delta v_{\min}\end{cases}. \tag{19}$$

In the following station-keeping simulations, the initial insertion error (3σ), navigation error (3σ), and maneuver error (1σ) are assumed to have normal distributions in the magnitude, and random distributions in the direction. All constraints discussed above and other parameters are listed in Table 3.

Table 3
The constraints and other parameters.

Parameters		Value
Initial insertion errors	Position	10 km
	Velocity	1 cm/s
Navigation errors	Position	1 km
	Velocity	1 cm/s
Maneuver errors		1%
Navigation/Impulse interval		2 days (2–60 days in Sect. 4.4)
Maneuver limitation	Minimum	1 cm/s
Orbital duration		2 years

4.2. Simulation results

In this subsection, the station-keeping simulations under practical constraints are conducted in the full ephemeris model. Both the station-keeping strategies introduced in Sect. 3 are applied to main nominal orbits in the Monte-Carlo simulations. To obtain reliable results, 200 sample points with random errors under practical constraints are generated for each Monte-Carlo simulation. Fig. 4 shows the trajectories of three main nominal orbits in the Moon-centred J2000 frame and the Moon-centred rotating frame during the station-keeping simulations with the DLQR control. The red stars in these figures are the locations of the target points with nonzero impulses.

Table 4 lists the station-keeping performances of three main nominal orbits with different station-keeping strategies. The annual cost is the average value of the station-keeping cost with one-year duration. The mean deviation and the maximum deviation are the average value and maximum value of position deviations in the Monte-Carlo simulation, respectively. The strategies in Table 4, TP (position), TP, DLQR, and DLQR (inf) refer to the target point method with consideration of only position deviation, the classic target point method with a comprehensive performance index, the previous DLQR control with a limited-form performance index, and the DLQR control with an infinite-form performance index, respectively. The slash in Table 4 means that the station-keeping failed at least once in the Monte-Carlo simulations.

As shown in Table 4, the 2:1 DRO and the halo (3) orbit can be maintained by all strategies, while the target point method failed in the station-keeping for the 9:2 NRHO. Among all four station-keeping strategies, two types of the DLQR control have shown lower cost, and two types of target point methods have shown lower position deviation. The mean position deviations of all strategies are lower than 2 km, and the maximum difference between different strategies is about 0.5 km. Thus, the DLQR control with limited-form, which has the lowest station-keeping cost, is preferred in this investigation.

Besides, the DLQR control with an infinite-form performance index in the station-keeping requires only the information about the current segment from the last target point to the current target point, which

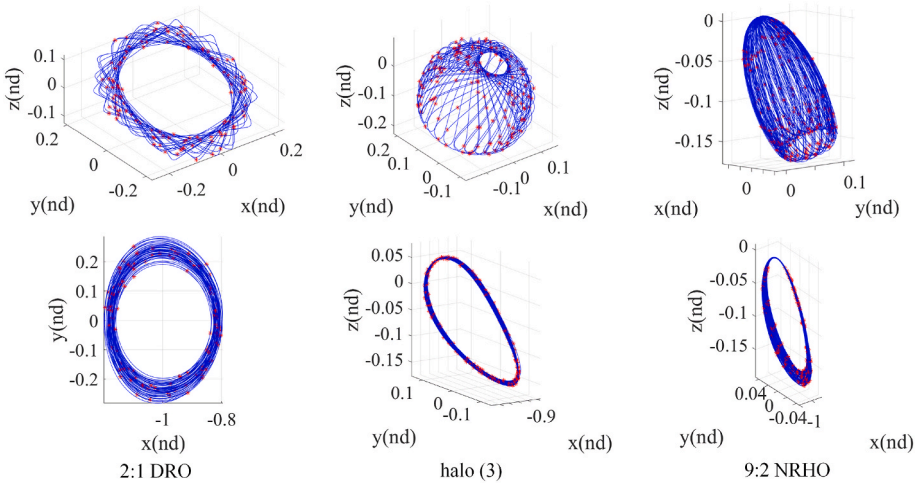

Fig. 4. The trajectories of three main nominal orbits in the Moon-centred J2000 frame (above) and the Moon-centred rotating frame (below) during the station-keeping simulations with the DLQR control.

Table 4
The performances of different station-keeping strategies on main nominal orbits.

Orbit	Period (days)	Stability index	Method	Annual cost (m/s)	Mean deviation (km)	Max deviation (km)
2:1 DRO	13.660	1	TP (pos)	1.6552	0.9259	3.6523
			TP	1.1231	1.1241	3.7497
			DLQR	0.8156	1.4754	4.4561
			DLQR (inf)	0.8478	1.4493	4.2812
halo (3)	13.349	51.584	TP (pos)	1.8872	0.9471	3.9243
			TP	1.8948	1.2252	4.5195
			DLQR	1.1494	1.4485	4.4378
			DLQR (inf)	1.3033	1.3575	4.1585
9:2 NRHO	6.562	1.319	TP (pos)	2.3427	1.1787	16.9397
			TP	/	/	/
			DLQR	1.6314	1.7240	17.7349
			DLQR (inf)	1.8516	1.6768	17.1940

means it is more flexible in the station-keeping process. As for the two target point methods, it has been observed that the target point method with consideration of the station-keeping cost failed at least once in the Monte-Carlo simulations with the 9:2 NRHO. When the 2:1 DRO is used as the nominal orbit, the annual station-keeping cost has been reduced more than 0.5 m/s by considering the station-keeping cost in the performance index.

Then, Hoeffding's inequality is exploited to estimate the accuracy of the annual costs and mean deviations. Hoeffding's inequality is given as,

$$P(|\overline{X} - E[\overline{X}]| \geq t) \leq 2\exp\left(\frac{2n^2t^2}{\sum_{i=1}^{n}(b_i - a_i)^2}\right), \tag{20}$$

where $\overline{X}$ is the average value of random variables, $E[\overline{X}]$ is the expectation value of random variables, a_i and b_i are the lower and upper limits of random variable values, t determines the width of the confidence interval, and n is the number of random variables. Actually, there are no theoretical lower and upper limits for the annual cost and mean deviation. Thus, the minimum and maximum values in the Monte-Carlo simulation are used as lower and upper limitations in Hoeffding's inequality. The number of trials in each Monte-Carlo simulation is $n = 200$.

The station-keeping performances of three main nominal orbits with the DLQR control are used as examples, and the results are listed in Table 5. The main nominal orbits have a low probability that the annual cost and mean deviation exceed the confidence intervals, which indicate that the station-keeping performances in Table 4 are valid. It is worth mentioning that the probability is sensitive to the width of the confidence interval. For the 2:1 DRO, the probabilities of the annual cost exceeding the expectation value by more than 0.05 m/s and 0.07 m/s are about 2.88% and 0.049%, respectively, and the probabilities of the mean deviation exceeding the expectation value by more than 0.03 km and 0.05 km are about 5.74% and 0.01%, respectively.

The 9:2 NRHO in Table 4 is obtained by differential correction, and actually the 9:2 NRHO can also be obtained by using the receding horizon method. When the DLQR control is used as the station-keeping strategy, the annual cost, mean deviation, and max deviation of the 9:2 NRHO obtained by the receding horizon method are 2.8275 m/s,

Table 5
The probability of the annual cost and mean deviation exceeding the confidence interval.

Orbit		Interval	Width of confidence interval/t	Probability
2:1 DRO	Annual cost	0.4483–0.9338 m/s	0.05 m/s	2.88%
	Mean deviation	1.3211–1.6395 km	0.03 km	5.74%
halo (3)	Annual cost	0.9957–1.3059 m/s	0.03 m/s	4.74%
	Mean deviation	1.3276–1.5961 km	0.03 km	1.35%
9:2 NRHO	Annual cost	1.2416–2.1645 m/s	0.1 m/s	1.83%
	Mean deviation	1.4866–2.0923 km	0.07 km	0.96%

Table 6
The station-keeping performances of different nominal orbits with the DLQR control.

Orbit	Period (days)	Stability index	Annual cost (m/s)	Mean deviation (km)	Max deviation (km)
DRO (1)	5.464	1	1.9570	1.6799	9.0081
DRO (2)	7.285	1	1.3769	1.5659	5.5565
DRO (3)	9.107	1	1.1476	1.4784	4.5833
DRO (4)	10.928	1	0.9928	1.4384	4.3947
DRO (5)	13.660	1	0.8156	1.4754	4.4561
halo (1)	14.583	349.022	1.2533	1.3518	4.3750
halo (2)	14.050	138.048	1.1894	1.4083	4.5706
halo (3)	13.349	51.584	1.1494	1.4485	4.4378
halo (4)	12.573	20.834	1.1704	1.4772	4.7680
halo (5)	11.771	17.326	1.1746	1.4786	4.7280
NRHO (1)	8.597	1.570	1.5899	1.7132	11.7657
NRHO (2)	7.956	1.693	1.8598	1.9347	17.8218
NRHO (3)	7.457	1.641	1.7957	1.9709	20.6822
NRHO (4)	6.562	1.319	1.6314	1.7240	17.7349
NRHO (5)	6.130	1.090	2.7771	2.1565	59.6839

2.2498 km, and 29.6125 km, respectively. The increase of annual cost is caused by discontinuities of the velocity in the nominal orbit. Thus, although the receding horizon method can be used to generate nominal orbits, it is more suitable to adopt the nominal orbit obtained by differential correction.

In order to provide comprehensive station-keeping performances of *cis*-lunar orbit families, the DLQR control is applied to all nominal orbits in the ephemeris model. The station-keeping performances of different nominal orbits are shown in Table 6. The difference of mean position deviation between nominal orbits of the same type are less than 0.5 km. The annual cost of DROs decrease with the increase of the period of DROs. When the period of halo orbits decreases, their stability indexes decrease gradually, the annual cost decreases first, and then increases slightly. NRHOs are members of the halo orbit family, and their annual costs do not show any tendency, but the annual cost of the NRHO (5) is significantly larger than that of other NRHOs.

The comparison between three types of nominal orbits shows that the DROs with large amplitudes have the lowest station-keeping cost, while the NRHOs generally have the highest cost. It is quite interesting that the unstable halo orbits could have lower station-keeping cost than the NRHOs and some DROs, indicating that the stability index has no direct effect on the station-keeping cost.

Table 7
The performances of the station-keeping on the nominal orbits constructed with different ephemeris models.

Orbit	Perturbation	Annual cost (m/s)	Mean deviation (km)	Max deviation (km)
2:1 DRO	None	0.8156	1.4754	4.4561
	SRP	7.1847	7.5923	10.3960
	NSLG	0.8106	1.4759	4.4216
halo (3)	None	1.1494	1.4485	4.4378
	SRP	6.5962	5.7505	8.3762
	NSLG	1.1486	1.4463	4.6059
9:2 NRHO	None	1.6314	1.7240	17.7349
	SRP	6.0373	3.7102	17.1725
	NSLG	3.6807	4.4594	19.8489

4.3. The effect of some perturbations

In the ephemeris model, some perturbations, such as the SRP and the nonspherical lunar gravity, are included. It would be meaningful to demonstrate their effects on the station-keeping performances, which could provide some valuable suggestions for future missions.

To study their effects, we have constructed the dynamical model without SRP, and the dynamical model without nonspherical lunar gravity. The low-fidelity nominal orbits in these dynamical models are constructed with differential correction. The DLQR control is used as the station-keeping strategy. Table 7 lists the performances of the station-keeping on the nominal orbits constructed with different ephemeris models. The NSLG in Table 7 is the abbreviation of nonspherical lunar gravity.

As shown in Table 7, the low-fidelity nominal orbits constructed in the ephemeris model without SRP have higher annual cost and position deviation. For DROs, the SRP increases the annual cost more than 6 m/s. Meanwhile, the increases of annual cost for halo orbit and NRHOs are lower. The SRP has increased the mean position deviation of nominal orbits with longer distances to the Moon, such as the 2:1 DRO and the halo (3) orbit. As for the nonspherical lunar gravity, its effect on the annual costs of the 2:1 DRO and the halo (3) orbit are less than 0.1 m/s, which is negligible. However, the nonspherical lunar gravity can increase the annual cost of the 9:2 NRHO more than 2 m/s, and also affect the position deviation observably, since the perilune of the 9:2 NRHO is very close to the Moon.

4.4. Station-keeping with different impulse intervals

In this subsection, different impulse intervals are considered to investigate their effects on the station-keeping cost and position deviation. The impulse interval is considered to be between 2 days and 60 days, and the navigation interval is chosen as the same value. The DLQ control is used as the station-keeping strategy in the Monte-Carlo simulation. In order to avoid the possible divergence caused by the initial insertion error, the first station-keeping impulse is applied 12 h after the insertion, and then station-keeping is conducted with specific impulse intervals. Fig. 5 shows the 2:1 DRO, halo (3) orbit and the 9:2 NRHO in the station-keeping simulations with 60 days, 10 days and 30 days as impulse intervals, respectively. The red stars are the target points where impulses are applied.

Table 8 lists the main quantities of the station-keeping simulation with different impulse intervals. Because of the distinct stability index, the 2:1 DRO and 9:2 NRHO can be maintained with impulse intervals of 60 days and 30 days, respectively, while the halo (3) orbit cannot be maintained with an impulse interval longer than 10 days. It is obvious that the nominal orbits with favourable stability, such as the 2:1 DRO and the 9:2 NRHO, normally require lower station-keeping cost when the impulse interval is longer, but the unstable halo orbits have an opposite tendency.

For the 2:1 DRO, with the increase of the impulse interval, the annual cost decreases but the position deviation increases. When the impulse interval increases to 15 days, the annual cost is only 0.1578 m/s, which is only 19% of the annual cost with a 2-day impulse interval. The annual cost can be decreased to 0.0501 m/s if the impulse interval is 60 days. However, the mean position deviation is 38.8173 km, which is much larger than the case of a 2-day impulse interval. For the 9:2 NRHO, when the impulse interval increases to 5 days, the annual cost has decreased more than 50%, and the position deviation is twice that of a 2-day impulse interval. The impulse interval of 15 days has shown a great station-keeping performance. The annual cost is 0.5184 m/s, much lower than other cases, and the position deviation is only 5.2904 km. As opposed to the nominal orbits with favourable stability, the station-keeping cost and position deviation of the halo (3) orbit have both obviously increased when the impulse interval is longer. When the impulse intervals are 2, 5, and 10 days, the annual costs of the halo orbit are

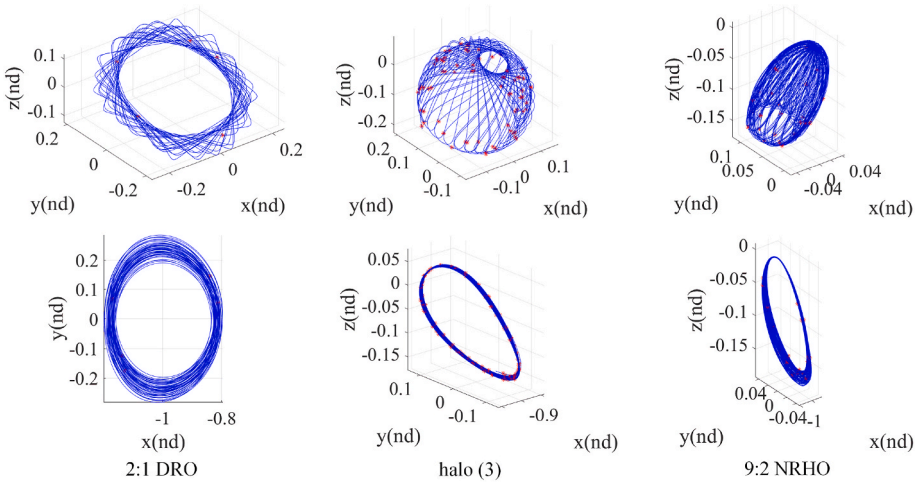

Fig. 5. The trajectories of three main nominal orbits in the Moon-centred J2000 frame (above) and the Moon-centred rotating frame (below) during the station-keeping simulation with long impulse intervals.

Table 8
The performances of the station-keeping with different impulse intervals.

Orbit	Stability index	Impulse interval (days)	Annual cost (m/s)	Mean deviation (km)	Max deviation (km)
2:1 DRO	1	2	0.8160	1.4764	4.2275
		5	0.8738	2.8034	10.3568
		10	0.3003	8.2300	34.5126
		15	0.1578	12.8807	44.7064
		30	0.2733	16.1809	59.7884
		60	0.0501	38.8173	114.0061
halo (3)	51.584	2	1.1484	1.4417	4.3373
		5	1.3633	2.9127	12.1523
		10	3.3968	17.3052	68.2160
		15	/	/	/
9:2 NRHO	1.319	2	1.9795	1.8959	31.0788
		5	0.9462	3.6719	35.4115
		10	0.9682	4.9101	38.8120
		15	0.5184	5.2904	18.7479
		30	1.1303	18.4035	54.6807
		60	/	/	/

1.1484, 1.3633, and 3.3968 m/s, respectively.

In conclusion, the increase of the impulse interval normally results in lower annual cost but higher position deviation for nominal orbits with favourable stability, and higher annual cost and position deviation for the unstable halo orbits. To achieve the balance between the annual cost and position deviation, it is necessary to investigate different impulse intervals for nominal orbits with favourable stability.

5. Conclusions

In this paper, different impulsive station-keeping strategies have been evaluated for the *cis*-lunar orbits in the full ephemeris model, including five DROs, five halo orbits, and five NRHOs. All nominal orbits are reconstructed in the full ephemeris model by using the differential correction and receding horizon method. Two strategies, the target point method and DLQR control, are evaluated by Monte-Carlo simulations. The comparison between different station-keeping strategies has shown that generally the DLQR control has the lowest station-keeping cost, and a slightly higher position deviation. The comparison between three types of nominal orbits shows that the DROs with large amplitudes have the lowest station-keeping cost, while the NRHOs generally have the highest cost. In addition, it has been found that the stability index has no direct effect on the station-keeping cost, and unstable halo orbits may have lower station-keeping cost than the NRHOs and some DROs.

The effects of SRP and nonspherical lunar gravity have also been assessed by constructing low-fidelity nominal orbits in dynamical models without SRP or non-spherical lunar gravity. The SRP have shown significant effects on the station-keeping cost and position deviation for all nominal orbits, whereas the nonspherical lunar gravity has significant effects only on the NRHOs because of the very low perilune.

To find suitable impulse intervals that can achieve a balance between the annual cost and position deviation, different impulse intervals between 2 days and 60 days are tested. The increase of the impulse interval results in lower annual cost but higher position deviation for stable DROs and weakly unstable NRHOs, whereas it causes both higher annual cost and position deviation for unstable halo orbits, indicating a strong dependency on the stability index of the nominal orbit. As a result, the DROs and NRHOs allow a much longer impulse interval than the unstable halo orbits.

The results can provide useful suggestions for selection of proper nominal orbits and station-keeping strategies for long-term lunar missions.

Declaration of competing interest

The authors declare that they do not have any commercial or associative interest that represents a conflict of interest in connection with the paper submitted.

Acknowledgements

The authors thank the Co-Editor for the careful review of the

manuscript. YW thanks the support of the National Natural Science Foundation of China (11872007) and the Fundamental Research Funds for the Central Universities. YS thanks the support of the National Natural Science Foundation of China (12003054). RZ thanks the support of the Academic Excellence Foundation of BUAA for PhD Students.

References

[1] M.L. Lidov, A family of spatial periodic orbits near the Moon and planets, Dokl. Akad. Nauk SSSR 223 (6) (1977) 1068–1071 (in Russian).
[2] J.V. Breakwell, J.V. Brown, The "halo" family of 3-dimensional periodic orbits in the Earth-Moon restricted 3-body problem, Celestial Mech. 20 (4) (1979) 389–404.
[3] D. Guzzetti, E.M. Zimovan, K. Howell, D. Davis, Stationkeeping analysis for spacecraft in lunar near rectilinear halo orbits, Adv. Astronaut. Sci. 160 (2017) 3199–3218.
[4] D. Davis, S. Bhatt, K. Howell, J. Jang, R. Whitley, F. Clark, D. Guzzetti, E. Zimovan, G. Barton, Orbit maintenance and navigation of human spacecraft at cislunar near rectilinear halo orbits, Adv. Astronaut. Sci. 160 (2017) 2257–2276.
[5] D.C. Davis, S.M. Phillips, K.C. Howell, S. Vutukuri, B. McCarthy, Stationkeeping and transfer trajectory design for spacecraft in cislunar space, Adv. Astronaut. Sci. 162 (2018) 3483–3502.
[6] L. Bucci, A. Colagrossi, M. Lavagna, Rendezvous in lunar near rectilinear halo orbits, Adv. Astronaut. Sci. Technol. 1 (1) (2018) 39–43.
[7] E.M. Zimovan, K.C. Howell, D.C. Davis, Near rectilinear halo orbits and their application in cis-lunar space, in: 3rd IAA Conference on Dynamics and Control of Space Systems, 2017, p. 20. Moscow, Russia.
[8] K. Boudad, K.C. Howell, D. Davis, Near rectilinear halo orbits in cislunar space within the context of the bicircular four-body problem, Adv. Astronaut. Sci. 174 (2021) 47–66.
[9] S. Trofimov, M. Shirobokov, A. Tselousova, M. Ovchinnikov, Transfers from near-rectilinear halo orbits to low-perilune orbits and the Moon's surface, Acta Astronaut. 167 (2020) 260–271.
[10] V. Muralidharan, K.C. Howell, Stationkeeping in Earth-Moon near rectilinear halo orbits, Adv. Astronaut. Sci. 175 (2021) 2743–2762.
[11] Y. Wang, R. Zhang, C. Zhang, H. Zhang, Transfers between NRHOs and DROs in the Earth-Moon system, Acta Astronaut. 186 (2021) 60–73.
[12] R.A. Broucke, Periodic Orbits in the Restricted Three Body Problem with Earth-Moon Masses, NASA-JPL Technical Report 32-1168, Jet Propulsion Laboratory, Pasadena, CA, 1968.
[13] M. Hénon, Numerical exploration of the restricted problem, V. Astron. Astrophys. 1 (1969) 223–238.
[14] M. Xu, S. Xu, Exploration of distant retrograde orbits around Moon, Acta Astronaut. 65 (5–6) (2009) 853–860.
[15] M. Vaquero, K.C. Howell, Leveraging resonant-orbit manifolds to design transfers between libration-point orbits, J. Guid. Control Dynam. 37 (4) (2014) 1143–1157.
[16] L. Capdevila, D. Guzzetti, K. Howell, Various transfer options from Earth into distant retrograde orbits in the vicinity of the Moon, Adv. Astronaut. Sci. 152 (2014) 3659–3678.
[17] R. Zhang, Y. Wang, H. Zhang, C. Zhang, Transfers from distant retrograde orbits to low lunar orbits, Celestial Mech. Dyn. Astron. 132 (2020) 41.
[18] R. Zhang, Y. Wang, C. Zhang, H. Zhang, The transfers from lunar DROs to Earth orbits via optimization in the four body problem, Astrophys. Space Sci. 366 (6) (2021) 1–16.
[19] L. Capdevila, K. Howell, A transfer network linking Earth, Moon, and the triangular libration point regions in the Earth-Moon system, Adv. Space Res. 62 (7) (2018) 1826–1852.
[20] W. Wiesel, W. Shelton, Modal control of an unstable periodic orbit, J. Astronaut. Sci. 31 (1983) 63–76.
[21] C. Simó, G. Gómez, J. Llibre, R. Martínez, J. Rodríguez, On the optimal station keeping control of halo orbits, Acta Astronaut. 15 (6–7) (1987) 391–397.
[22] G. Gómez, K.C. Howell, J. Masdemont, C. Simó, Station-keeping strategies for translunar libration point orbits, Adv. Astronaut. Sci. 99 (2) (1998) 949–967.
[23] K.C. Howell, H.J. Pernicka, Station-keeping method for libration point trajectories, J. Guid. Control Dynam. 16 (1) (1993) 151–159.
[24] T.A. Pavlak, K.C. Howell, Strategy for long-term libration point orbit stationkeeping in the Earth–Moon system, Adv. Astronaut. Sci. 142 (2012) 1717–1734.
[25] D.C. Folta, T.A. Pavlak, A.F. Haapala, K.C. Howell, M. Woodard, Earth–Moon libration point orbit stationkeeping: theory, modeling, and operations, Acta Astronaut. 94 (1) (2014) 421–433.
[26] Y. Lian, G. Gómez, J.J. Masdemont, G. Tang, Station-keeping of real Earth–Moon libration point orbits using discrete-time sliding mode control, Commun. Nonlinear Sci. Numer. Simulat. 19 (10) (2014) 3792–3807.
[27] M. Shirobokov, S. Trofimov, M. Ovchinnikov, Survey of station-keeping techniques for libration point orbits, J. Guid. Control Dynam. 40 (5) (2017) 1085–1105.
[28] H. Zhang, S. Li, Station-keeping of libration point orbits by means of projecting to the manifolds, Acta Astronaut. 163 (2019) 38–44.
[29] Y. Qi, A. de Ruiter, Station-keeping strategy for real translunar libration point orbits using continuous thrust, Aero. Sci. Technol. 94 (2019), 105376.
[30] A. Farrés, D. Folta, C. Webster, Using spherical harmonics to model solar radiation pressure accelerations, Adv. Astronaut. Sci. 162 (2018) 3365–3383.
[32] B.G. Marchand, K.C. Howell, R.S. Wilson, Improved corrections process for constrained trajectory design in the n-body problem, J. Spacecraft Rockets 44 (4) (2007) 884–897.
[33] J. Williams, D.E. Lee, R.J. Whitley, K.A. Bokelmann, D.C. Davis, C.F. Berry, Targeting cislunar near rectilinear halo orbits for human space exploration, Adv. Astronaut. Sci. 160 (2017) 3125–3144.